FACILITATED TRANSPORT OF OXYGEN IN THE PRESENCE OF MEMBRANES IN THE DIFFUSION PATH

JOSE M. GONZALEZ-FERNANDEZ and SUSIE E. ATTA
Mathematical Research Branch, National Institute of Arthritis, Diabetes, Digestive, and Kidney Diseases, National Institutes of Health, Bethesda, Maryland 20205

ABSTRACT Most of the experimental observations on facilitated transport have been done with millipore filters, and all the theoretical studies have assumed homogeneous spatial properties. In striated muscle there exist membranes that may impede the diffusion of the carrier myoglobin. In this paper a theoretical study is undertaken to analyze the transport in the presence of membranes in the diffusion path. For the numerical computations physiologically relevant values of the parameters were chosen. The numerical results indicate that the presence of membranes tends to decrease the facilitation. For the nonlinear chemical kinetics of the reaction of oxygen with the carrier, this decrement also depends on the location of the membranes. At the higher oxygen concentration side of each membrane the flow of combined oxygen is transferred to the flow of dissolved oxygen. The reverse process occurs at the lower concentration side. Jump discontinuities of the concentration of the oxygen-carrier compound at each membrane are associated with these transfers. The decrement of facilitation is due to the cumulative effect of these jump discontinuities.

INTRODUCTION

Wittenberg (35) and Scholander (29) showed experimentally that the presence of hemoglobin or myoglobin in solution enhances the transport of oxygen. The influence of the physical and chemical parameters associated with this facilitated transport have been further examined experimentally (36). Recently Wittenberg et al. (38) have provided experimental evidence that this mechanism is operative in striated muscle. The bulk of the evidence, experimental (36) and theoretical (17, 20, 28, 39), supports the notion that the total flow of oxygen is the additive result of the diffusion of the free oxygen and the diffusion of the oxygen-carrier compound. The latter determines the facilitated part of the transport. In striated muscle, however, there exist membranes (the sarcoplasmic reticulum (26) and the muscle fiber membrane) that may impede the diffusion of the protein carrier. The presence of a membrane impermeable to the carrier abolishes the diffusion of the oxygen-carrier compound at that place. Since the oxygen can diffuse through the membrane only as free oxygen, this would necessitate that the flow of combined oxygen be transferred to the flow of free oxygen on one side of the membrane and transferred back to the flow of combined oxygen on the other side. The purpose of this report is to determine whether this process occurs and how much the resulting facilitation depends on the parameters of the process.

GLOSSARY

z	space variable, cm
ℓ	thickness of the slab, cm
O	oxygen
P	myoglobin
OP	oxymyoglobin
x_1	concentration of free oxygen, mol cm^{-3}
y_1	concentration of free oxygen (approximation), mol cm^{-3}
x_2	concentration of oxymyoglobin, mol cm^{-3}
y_2	concentration of oxymyoglobin (approximation), mol cm^{-3}
C_p	total concentration of myoglobin, reduced and oxygenated, mol cm^{-3}
k'	association rate coefficient (nonlinear chemical kinetics), cm^3 mol^{-1} s^{-1}
k	dissociation rate coefficient (nonlinear chemical kinetics), s^{-1}
k_1	association rate coefficient (linear chemical kinetics), s^{-1}
k_2	dissociation rate coefficient (linear chemical kinetics), s^{-1}
a	constant term (linear chemical kinetics), mol cm^{-3} s^{-1}
D_1	diffusion coefficient for free oxygen, cm^2 s^{-1}
D_2	diffusion coefficient for oxymyoglobin, cm^2 s^{-1}
x_1^0	$x_1(0)$, mol cm^{-3}
x_1^ℓ	$x_1(\ell)$, mol cm^{-3}
F_{nf}	nonfacilitated flow, mol cm^{-2} s^{-1}
F_f	facilitated flow, mol cm^{-2} s^{-1}
F	total flow, mol cm^{-2} s^{-1}
F_d	flow of free oxygen, mol cm^{-2} s^{-1}
F_c	flow of combined oxygen, mol cm^{-2} s^{-1}
$x_2^{eq}(x_1)$	concentration of oxymyoglobin in equilibrium with x_1, mol cm^{-3}
n	number of interior membranes
z_i	location of the i^{th} interior membrane, cm
δ	intermembrane distance, cm
α	oxygen solubility coefficient, mol cm^{-3} torr^{-1}
$f\|_{x_1^j}$	or
$f(z_i^\pm)$	stands for $\lim f(z_i \pm \epsilon)$ as $\epsilon > 0 \to 0$
Δ_i^+	$= x_2^{eq}[x_1(z_i)] - x_2(z_i^+)$, mol cm^{-3}
Δ_i^-	$= x_2(z_i^-) - x_2^{eq}[x_1(z_i)]$, mol cm^{-3}
x_1^j	$j = 1, \ldots, I$ subset from $x_1^\ell \le x_1 \le x_1^0$
ζ_j	value of z such that $x_1(\zeta_j) = x_1^j$
x_2^j	$= x_2(\zeta_j)$

χ_i $= x_1(z_i)$
$\hat{\chi}_j$ approximation to ζ_j
$\hat{x}_2^j$ approximation to x_2^j
$\hat{\chi}_i$ approximation to χ_i
x_1^{*j} some value of x_1 in the interval $x_1^j > x_1 > x_1^{j+1}$
x_2^{*j} $= x_2^{eq}(x_1^{*j})$

To conform with the current usage in the physiological literature the concentration of free oxygen and the distance will be expressed in torr and micrometers, respectively, in the description of the results.

THE MODEL AND THE NUMERICAL METHOD

The experimental setup, as reported in the literature (29, 35, 36), consisted essentially of a slab (millipore filter) of known thickness and area containing a solution of the protein. This slab separated two gas chambers that contained mixtures of oxygen kept at constant partial pressures. The resulting steady-state flow of oxygen across the slab was measured.

The theoretical model that we studied incorporates these basic features plus a spatial inhomogeneity by assuming the existence of membranes inside the body of the slab. These membranes are impermeable to the protein carrier but they are no different than the rest of the space in regard to the diffusion of oxygen.

Consider a region of space $0 \le z \le \ell$ containing oxygen (O), myoglobin (P) and oxymyoglobin (OP) in solution. Let x_1 and x_2 be the concentration of O and of OP, respectively. Let C_p be the total concentration of P, reduced and oxygenated. If one assumes that the diffusion coefficient of OP and of P are essentially the same, one can consider that C_p is a constant (11). Let D_1 and D_2 be the diffusion coefficients of O and P, respectively. The chemical reactions taking place are assumed to be

$$O + P \underset{k}{\overset{k'}{\rightleftharpoons}} OP$$

where k' and k are the association and dissociation rate coefficients, respectively.

Let the membranes be located at z_i, $i = 1, \ldots, n$ with $z_i < z_{i+1}$, and let $z_0 = 0$ and $z_{n+1} = \ell$. D_2 is assumed to be the same positive constant in the subintervals $z_i < z < z_{i+1}$ and zero at the points z_i, $i = 0, 1, \ldots, n+1$. D_1 is assumed to be a positive constant throughout. One assumes that the system is in a steady state and that

$$D_1 \frac{d^2x_1}{dz^2} = k'x_1(C_p - x_2) - kx_2 \tag{1}$$

and

$$D_2 \frac{d^2x_2}{dz^2} = -k'x_1(C_p - x_2) + kx_2 \tag{2}$$

are satisfied inside every subinterval $z_i < z < z_{i+1}$. The following notation will be used. If $f(z)$ is a function of z, let $f|_{z_i^+}$ or $f(z_i^+)$ stand for the lim $f(z_i \pm \epsilon)$ as $\epsilon > 0 \to 0$. To satisfy the requirements at the membranes the following conditions are introduced:

$$\left.\frac{dx_2}{dz}\right|_{z=z_i^-} = \left.\frac{dx_2}{dz}\right|_{z=z_i^+} = 0 \tag{3}$$

and

$$x_1|_{z=z_i^-} = x_1|_{z=z_i^+} \tag{4}$$

$$\left.\frac{dx_1}{dz}\right|_{z=z_i^-} = \left.\frac{dx_1}{dz}\right|_{z=z_i^+} \tag{5}$$

for $i = 1, 2, \ldots, n$.

The boundary conditions are

$$x_1(0) = x_1^0,\ x_1(\ell) = x_1^\ell \tag{6}$$

and

$$\left.\frac{dx_2}{dz}\right|_{z=0} = \left.\frac{dx_2}{dz}\right|_{z=\ell} = 0. \tag{7}$$

Without loss of generality one can assume that $x_1^0 > x_1^\ell \ge 0$.

In what follows, the term membrane will include the membranes at the boundaries. When a specific reference to a membrane inside the slab is needed, the term interior membrane will be used.

The solution for this problem is approximated by using a slight generalization of the piecewise analytic technique that we developed in a previous paper (8). In this paper we will present a description of the numerical method, with attention to the features needed to take care of the presence of interior membranes.

First, a partition of the interval $x_1^\ell \le x_1 \le x_1^0$ will be defined. Consider a set x_1^j, $j = 1, 2, \ldots, I$ such that $x_1^0 = x_1^1 > x_1^2 > \ldots > x_1^I = x_1^\ell$. Assign the index j to the subinterval $x_1^{j+1} < x_1 < x_1^j$. For this subinterval, consider the linear system

$$D_1 \frac{d^2y_1}{dz^2} = k_1y_1 - k_2y_2 + a \tag{8}$$

$$D_2 \frac{d^2y_2}{dz^2} = -k_1y_1 + k_2y_2 - a \tag{9}$$

obtained by expanding the right sides of Eqs. 1 and 2 about x_1^*, x_2^* where $x_1^{j+1} < x_1^* < x_1^j$ and $x_2^* = C_pk'x_1^*/(k'x_1^* + k)$. One can verify that $k_1 = C_pk'k/(k'x_1^* + k)$, $k_2 = k'x_1^* + k)$ and $a = C_p(k'x_1^*)^2/(k'x_1^* + k)$.

Consider now the functions $x_1(z)$ and $x_2(z)$ that satisfy Eqs. 1 and 2, the interphase conditions (Eqs. 3–5), and the boundary conditions (Eqs. 6 and 7). Assume that $x_1(z)$ is monotonically decreasing on $0 \le z \le \ell$. The partition x_1^j, $j = 1, 2, \ldots, I$, should satisfy the subsidiary conditon that no x_1^j is a value of $x_1(z)$ at a membrane. For every $j = 2, \ldots, I-1$ define ζ_j by $x_1(\zeta_j) = x_1^j$. The partition x_1^j, $j = 1, \ldots, I$, should be fine enough so that for every pair z_i, z_{i+1}, $i = 0, 1, \ldots, n$, there should be at least one ζ_j, such that $z_i < \zeta_j < z_{i+1}$. In addition, let $x_2^j = x_2(\zeta_j)$, $j = 2, \ldots, I-1$, and let $\chi_i = x_1(z_i)$, $i = 1, \ldots, n$.

Let $\hat{\zeta}_j$, $\hat{x}_2^j$, $j = 2, \ldots, I-1$, and $\hat{\chi}_i$, $i = 1, \ldots, n$, be the approximations to ζ_j, x_2^j, $j = 2, \ldots, I-1$, and χ_i, $i = 1, \ldots, n$, respectively. Next a piecewise analytic representation will be defined on the interval $0 \le z \le \ell$. Let $\hat{\zeta}_1 = 0$ and $\hat{\zeta}_I = \ell$. Consider the partition of $0 \le z \le \ell$ defined by the union of $\hat{\zeta}_j$, $j = 1, \ldots, I$, and z_i, $i = 1, \ldots, n$. Observe that each subinterval of this partition is contained in, or is itself, some $\hat{\zeta}_j \le z \le \hat{\zeta}_{j+1}$. Assign this j to this subinterval. On this subinterval the system (Eqs. 1 and 2) is replaced by the system (Eqs. 8 and 9).

For subintervals $\hat{\zeta}_j \le z \le \hat{\zeta}_{j+1}$ of the partition that do not have a membrane at one of its end points, the approximation $y_1(z)$, $y_2(z)$ is the solution of Eqs. 8 and 9 satisfying the boundary conditions

$$y_1(\hat{\zeta}_j) = x_1^j, \qquad y_1(\hat{\zeta}_{j+1}) = x_1^{j+1},$$
$$y_2(\hat{\zeta}_j) = \hat{x}_2^j, \qquad y_2(\hat{\zeta}_{j+1}) = \hat{x}_2^{j+1}.$$

For subintervals that have a membrane at one of its end points, say the subinterval $\hat{\zeta}_j \le z \le z_i$, the approximation $y_1(z)$, $y_2(z)$ is the solution of Eqs. 8 and 9 satisfying the boundary conditions

$$y_1(\hat{\zeta}_j) = x_1^j, \qquad y_1(z_i) = \hat{\chi}_i,$$
$$y_2(\hat{\zeta}_j) = \hat{x}_2^j, \qquad \left.\frac{dy_2}{dz}\right|_{z_i^-} = 0.$$

The solutions of these problems are analytic functions that can be expressed in a closed form.

Since the slab is assumed to contain no sinks or sources, then the following matching flow conditions are demanded:

$$\left.\frac{dy_k}{dz}\right|_{z=\hat{\xi}_j^-} - \left.\frac{dy_k}{dz}\right|_{z=\hat{\xi}_j^+} = 0, \qquad k = 1, 2, j = 2, \ldots, I-1,$$

and

$$\left.\frac{dy_1}{dz}\right|_{z=z_i^-} - \left.\frac{dy_1}{dz}\right|_{z=z_i^+} = 0, \qquad i = 1, \ldots, n.$$

These conditions establish how the piecewise solutions should be joined to each other at the partition points of the interval $0 \le z \le \ell$. The $2(I-2) + n$ variables $\hat{\xi}_j, \hat{x}_2^j, j = 2, \ldots, I-1$, and $\hat{\chi}_i, i = 1, \ldots, n$, should satisfy the $2(I-2) + n$ matching flow conditions above. One may solve this nonlinear system by some numerical method such as the Newton method. Advantage can be taken of the fact that the Jacobian matrices appearing in the linear steps of the Newton method have analytic expressions.

Consider a point x_1, x_2 that belongs to a solution of Eqs. 1 and 2. One can show (8) that the error between the values given by the operator (Eqs. 1 and 2), and the approximating operator (Eqs. 8 and 9) are bounded by

$$k'C_p \max_{j=2,\ldots,I} (x_1^{j-1} - x_1^j)$$

uniformly on $x_1^\ell \le x_1 \le x_1^0$. Since the boundary conditions at $z = 0$ and at $z = \ell$ coincide for the correct and the approximating problem, one can expect that the approximating solutions will tend to the correct solution as the term $\max (x_1^{j-1} - x_1^j), j = 2, \ldots, I$, of the error bound decreases as I increases.

For each problem studied several sets $x_1^j, j = 1, \ldots, I$, from $x_1^\ell \le x_1 \le x_1^0$ with increasing I were used to assess the convergence of the approximating solutions with the refinement of the partitions.

For the transport in a slab with no interior membranes, the numerical results agreed well with the ones obtained by Rubinow and Dembo (28) and Kutchai et al. (20). When interior membranes are present, no numerical results have been found in the literature. However, we have developed an independent algebraic method that will be presented in a forthcoming report. A comparison of the results obtained by the present method and by the algebraic method was found to be very satisfactory.

This model does not take into account the oxygen consumption present in the muscle. The results, however, may give a preliminary insight into the in vivo situation. A model that incorporates oxygen consumption is being developed by the authors.

NUMERICAL RESULTS

Features of the Solutions Due to the Presence of Membranes

Let F denote the total flow of oxygen. Define the nonfacilitated flow by

$$F_{nf} = D_1 \frac{x_1^0 - x_1^\ell}{\ell} \tag{10}$$

and the facilitated flow by

$$F_f = F - F_{nf}. \tag{11}$$

By adding Eqs. 1 and 2 and integrating the following constant is obtained:

$$F = -D_1 \, dx_1/dz - D_2 \, dx_2/dz. \tag{12}$$

At each point z let $F_d = -D_1 \, dx_1/dz$ denote the flow of dissolved oxygen and $F_c = -D_2 dx_2/dz$ denote the flow of combined oxygen. Then $F = F_d + F_c$; at every point the total flow is apportioned between the free and the combined form.

It is useful to introduce the following reference function

$$x_2^{eq}(x_1) = C_p \frac{k'x_1}{k + k'x_1}.$$

This expression is used to rewrite the right-hand side of Eq. 2 as the product $(k + k'x_1)\,[x_2 - x_2^{eq}(x_1)]$ which can be viewed as a chemical conductance coefficient times a chemical gradient. The function $x_2 - x_2^{eq}(x_1)$ expresses at each location the difference between the actual oxymyoglobin concentration x_2 and the concentration $x_2^{eq}(x_1)$ that would exist in equilibrium with the dissolved oxygen concentration x_1 at that location. An expression for the flow of oxygen transferred from the dissolved to the combined form on an interval $z' < z < z''$ may be obtained by integrating Eq. 2,

$$F_c(z'') - F_c(z') = \int_{z'}^{z''} (k'x_1 + k) \{x_2^{eq}[x_1(z)] - x_2(z)\} dz. \tag{13}$$

One observes that for large values of x_1 the same transfer of flows can be attained with a smaller departure from equilibrium.

For the computations it is desirable to choose values for the parameters that are representative of the ones occurring in striated muscle in vivo. Table I lists the values considered for the numerical computations. The amount of computations needed to cover all the possible combinations of those values is prohibitively large. Therefore for each question studied a particular selection of values was made. The results obtained were complemented by obtaining additional solutions for some other values of the parameters.

Furthermore, the suitability for the in vivo situation of the values available in the literature is somewhat tentative. Moll (23) considers that the value 2.7×10^{-7} cm^2 s^{-1} that he obtained for D_2 in muscle homogenates is probably an upper bound for the one in intact cells. The values k' and k have been obtained only in vitro. Since the myoglobin is a water-soluble protein apparently not bound to tissue structures, the model assumes a uniform concentration of this protein. However, Goldfisher (7) found myoglobin largely confined to the A band of the muscle fiber. James (13), on the other hand, found myoglobin uniformly distributed within the muscle cell. James (13) has shown that formaldehyde fixation, used by Goldfisher, appears not to be an appropriate technique for the purpose of studying the distribution of myoglobin in muscle cells. Morita et al. (24) confirmed James's conclusions. Wittenberg (37) observed that if myoglobin is excluded from the mitochondria, then the average concentration outside of the mitochondria

TABLE I
VALUES OF THE PARAMETERS FOR STRIATED MUSCLE AT 37°C

Parameter	Value	Reference
D_1	$1.26 \times 10^{-5}, \ldots, 1.5 \times 10^{-5}$ cm^2 s^{-1}	10, 16, 18, 19, 22, 33
D_2	$2.0 \times 10^{-7}, \ldots, 2.7 \times 10^{-7}$ cm^2 s^{-1}	23, 37
k'	2.4×10^{10} cm^3 mol^{-1} s^{-1}	1, 37
k	65.0 s^{-1}	1, 37
C_p	$4.46 \times 10^{-7}, \ldots, 3.57 \times 10^{-6}$ mol cm^{-3}	37 (Table III; page 594)
α	1.35×10^{-9} mol cm^{-3} torr^{-1}	10, 30
x_1^0	$1.35 \times 10^{-8}, \ldots, 5.4 \times 10^{-8}$ mol cm^{-3}	6
x_1^ℓ	$5.4 \times 10^{-11}, \ldots, 6.75 \times 10^{-9}$ mol cm^{-3}	2, 3, 14, 15, 31
ℓ	$5.0 \times 10^{-4}, \ldots, 3.6 \times 10^{-2}$ cm	12, 19, 21, 25, 27, 37 (Table IV)

To express the numerical results the concentration of oxygen will be given in torr and the distance will be given in micrometers; this is to conform with the units commonly used in the literature. The value 1.35×10^{-9} mol cm^{-3} torr^{-1} was used for the oxygen solubility (α) at 37°C (10, 30).

would be of the order of 1.5-fold greater than the one reported for the total volume of tissue. Furthermore, the local concentration would still be larger if one excluded the volume preempted by the contractile apparatus. The parameter x_1^ℓ represents the partial pressure of oxygen at the low end of the diffusion path; the experimentally measured values of its physiological correlate in vivo appear to vary widely, from ~20 torr down to a fraction of 1 torr (2, 31, 34, 9). However, the measured extracellular p_{O_2} associated with a limitation of oxygen consumption may not be at the end of the diffusion path (31, 4). On the other hand, even though the limiting value of p_{O_2} for mitochondria in vitro is only a fraction of 1 torr (3, 32) it is not certain whether this can be extrapolated to the in vivo situation (5).

Within the limitations that attend the above uncertain-

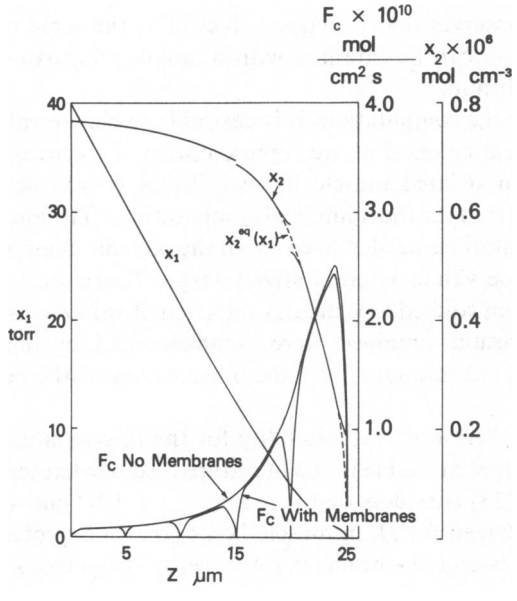

FIGURE 1 Profiles of $x_1(z)$, $x_2(z)$, and $F_c(z)$ inside a slab with four interior membranes. $C_p = 8.92 \times 10^{-7}$ mol cm^{-3}, $D_1 = 1.5 \times 10^{-5}$ cm^2 s^{-1}, $D_2 = 2.7 \times 10^{-7}$ cm^2 s^{-1}, $x_1^0 = 40$ torr, $x_1^\ell = 0.1$ torr, and $\ell = 25$ μm. The values of the other parameters k', k, and α are listed in Table I. For comparison purposes the profile of F_c for no interior membranes is also graphed. The values of $x_2^{eq}(x_1)$ are also graphed, dashed lines, about $z = 20$ and $z = 25$ μm. The profile of $x_1(z)$ is steeper in the intervals around the membranes where F_c changes rapidly, however this is not apparent in the graphs because of the lack of resolution of the scale used. For no interior membranes $F = 3.922 \times 10^{-10}$ mol cm^{-2} s^{-1} and $F_f = 6.90 \times 10^{-11}$ mol cm^{-2} s^{-1}. For four interior membranes $F = 3.861 \times 10^{-10}$ mol cm^{-2} s^{-1} and $F_f = 6.292 \times 10^{-11}$ mol cm^{-2} s^{-1}. This amounts to a 9% decrement in the facilitated flow.

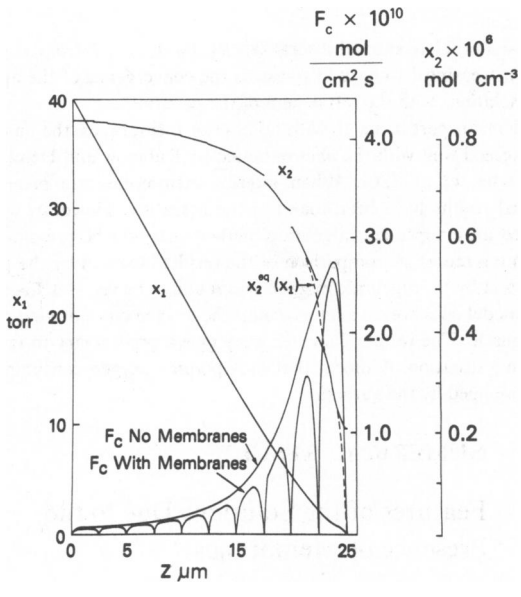

FIGURE 2 The same display as in Fig. 1 for nine interior membranes. $C_p = 8.92 \times 10^{-7}$ mol cm^{-3}, $D_1 = 1.5 \times 10^{-5}$ cm^2 s^{-1}, $D_2 = 2.7 \times 10^{-7}$ cm^2 s^{-1}, $x_1^0 = 40$ torr, $x_1^\ell = 0.1$ torr, and $\ell = 25$ μm. The values of the other parameters k', k and α are listed in Table I. For comparison purposes the profile of $F_c(z)$ for no interior membranes is also graphed. The values of $x_2^{eq}(x_1)$ are also graphed, dashed lines, around $z = 22.5$ and $z = 25$ μm. The profile of $x_1(z)$ is steeper in the intervals around the membranes where $F_c(z)$ changes rapidly, however this is not apparent in the graphs because of the lack of resolution of the scale used. For no interior membranes $F = 3.922 \times 10^{-10}$ mol cm^{-2} s^{-1} and $F_f = 6.90 \times 10^{-11}$ mol cm^{-2} s^{-1}. For nine interior membranes $F = 3.726 \times 10^{-10}$ mol cm^{-2} s^{-1} and $F_f = 4.940 \times 10^{-11}$ mol cm^{-2} s^{-1}. This amounts to a 28% decrement in the facilitated flow.

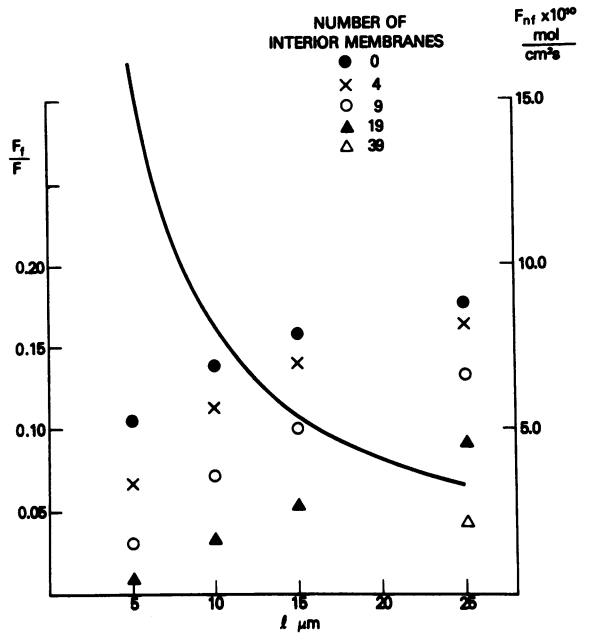

FIGURE 3 Dependence of F_f/F on the thickness of the slab and on the number of interior membranes. The membranes are equally spaced. $C_p = 8.92 \times 10^{-7}$ mol cm^{-3}, $D_1 = 1.5 \times 10^{-5}$ cm^2 s^{-1}, $D_2 = 2.7 \times 10^{-7}$ cm^2 s^{-1}, $x_1^0 = 40$ torr and $x_1^\ell = 0.1$ torr. The values of the other parameters k', k and α are listed in Table I. The solid line represents the values of F_{nf}.

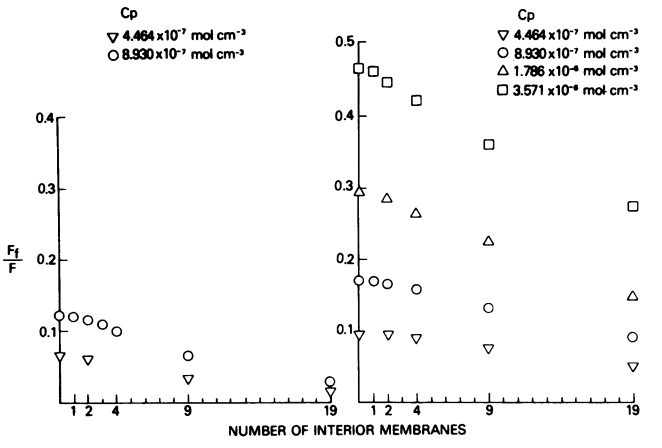

FIGURE 4 Dependence of the relationship between F_f/F and the number of interior membranes on the concentration C_p of the carrier. The membranes are equally spaced. For the left panel $\ell = 10$ μm and $x_1^\ell = 0.5$ torr; for the right panel $\ell = 25$ μm and $x_1^\ell = 0.1$ torr; for both $x_1^0 = 40$ torr. The values of D_1 and D_2 used are listed in Table III. The values of the other parameters k', k and α are listed in Table I.

ties the numerical results that follow may give some initial estimates on the effect that membranes in the diffusion path have on the facilitated transport.

The profiles of the concentrations x_1 and x_2 and the flow F_c that were obtained for six equally spaced membranes are represented in Fig. 1. The solution $x_2(z)$ exhibits jump discontinuities at every membrane site. For comparison purposes the flow F_c when no interior membranes were present is also graphed. One can observe that at every membrane the value of F_c is zero: the oxygen flow there is supported entirely by the dissolved oxygen. The rapid changes in F_c are concentrated in small intervals around the membrane sites. The values of F_c elsewhere differ little from the values obtained for no membranes. The differences $x_2 - x_2^{eq}(x_1)$ follow those changes *pari passu*, (cf. Eq. 13). Figs. 1 and 2 show the progressive changes when the number of membranes increases.

Dependence of Facilitation on the Values of the Parameters Pertaining to Striated Muscle In Vivo

Fig. 3 displays the ratio F_f/F as a function of the thickness ℓ of the slab and the number of interior membranes. The values of the nonfacilitated flow (F_{nf}) are also graphed so that the actual values of the facilitated flow (F_f) and the total flow (F) can be obtained from the values of F_f/F.

In view of the uncertainty of what the proper value or range of values of x_1^ℓ should be, the results of fig. 3 were complemented by performing a number of computations with values of x_1^ℓ ranging from 0.04 to 5 torr; the resulting values of F_f/F are listed in Table II.

For equally spaced membranes, Fig. 4 shows the dependence of F_f/F on the number of membranes for $\ell = 10$ and $\ell = 25$ μm and values of C_p ranging from 4.464×10^{-7} mol cm^{-3} to 3.571×10^{-6} mol cm^{-3}. The value 4.464×10^{-7}

TABLE II
DEPENDENCE OF F_f/F ON THE NUMBER n OF INTERIOR MEMBRANES FOR DIFFERENT VALUES OF ℓ AND x_1^ℓ.

	$\ell = 10$ μm			$\ell = 25$ μm		
n	$x_1^\ell = 0.1$ torr	0.5 torr	5 torr	$x_1^\ell = 0.04$ torr	0.1 torr	5 torr
0	0.140	0.127	0.0644	0.179	0.176	0.0701
4	0.113	0.106	0.0546	0.166	0.163	0.0666
9	0.0731	0.0663	0.0391	0.138	0.132	0.0589
19	0.0313	0.0295	0.00728	0.0918	0.0904	0.0453
39				0.0441	0.0434	

$C_p = 8.92 \times 10^{-7}$ mol cm^{-3}, $D_1 = 1.5 \times 10^{-5}$ cm^2 s^{-1}, $D_2 = 2.7 \times 10^{-7}$ cm^2 s^{-1}, $x_1^0 = 40$ torr. The values of the other parameters k', k, and α are listed in Table I. The membranes are equally spaced.

TABLE III
VALUES OF D_1 AND D_2 (USED TO COMPUTE THE RESULTS OF FIG. 4) THAT CORRESPOND TO DIFFERENT VALUES OF MYOGLOBIN CONCENTRATION C_p

$C_p \times 10^7$ mol cm^{-3}	$D_1 \times 10^5$ cm^2 s^{-1}	$D_2 \times 10^7$ cm^2 s^{-1}
4.464	1.50	2.70
8.93	1.46	2.50
17.86	1.39	2.35
35.71	1.26	2.20

mol cm^{-3} corresponds to an upper-bound concentration of myoglobin in striated muscle of dog, horse, and man; the value 3.571×10^{-6} mol cm^{-3} corresponds to the concentration of myoglobin in the muscles of diving animals (37). For this range of carrier concentrations a further uncertainty on the values of D_1 and D_2 was present because these values depend also on the protein concentration. The values of D_1 and D_2 used in the above computations for the different values of muscle myoglobin concentrations were calculated in the following manner. For $C_p = 4.467 \times 10^{-7}$ mol cm^{-3} D_1 was set to 1.5×10^{-5} cm^2 s^{-1} (10, 16, 18) and D_2 was set to 2.7×10^{-7} cm^2 s^{-1} (23). For carrier concentrations larger than $C_p = 4.467 \times 10^{-7}$ mol cm^{-3} the values of D_1 and D_2 were adjusted by using the experimental relationships between changes in D_1 and D_2 associated with changes in C_p as given by Wittenberg (37; Figs. 8 and 10). The resulting values are listed in Table III.

Influence of the Location of the Membranes

To illustrate the dependence of the facilitation on the location of the membranes the facilitated flow was computed for two different arrangements of membrane locations. The slab thickness was 10 μm. In one instance, five interior membranes were located at z = 0.5, 1.0, 1.5, 2.0, and 2.5 μm. In the other instance, the locations were z = 7.5, 8.0, 8.5, 9.0, and 9.5 μm. In this manner the number of membranes and the set of intermembrane distances were invariant. The results listed in Table IV show that the decrement in facilitation is larger when the membranes are located near the low oxygen boundary.

For the membranes near $z = 0$ the resulting values of x_1 at the interior membranes were 37.8, 35.5, 33.3, 31.1, and 28.8 torr; for the membranes near $z = \ell$, those values were 10.1, 8.12, 6.14, 4.20, and 2.30 torr.

Influence of the Values of the Parameters Pertaining to Some In Vitro Experiments in Striated Muscle

Wittenberg et al. (38) have measured in vitro the oxygen uptake by bundles of muscle fibers at 37°C teased from pigeon breast muscle. The bundles were immersed in an environment of controlled oxygen concentration. It was found that for low environmental oxygen concentration the presence of functional myoglobin contributes to the oxygen uptake by the muscle. The bundles were ~ 500 μm in diameter and the muscle fiber sizes were homogeneous and ~ 30 μm in diameter. This implies that the average diffusion path may cross about eight muscle fibers. One may ask to what extent the presence of the cell membranes may interfere with a possible facilitated transport. To obtain a preliminary answer to this question and to study the dependence of the transport on the values of the parameters, the facilitated transport was computed for all combinations of the following parameter values: ℓ = 180 and 360 μm; x_1^0 = 10 and 40 torr; x_1^ℓ = 0, 0.1, and 1.0 torr; $D_2 = 2.0 \times 10^{-7}$ and 2.7×10^{-7} cm^2 s^{-1}; $\delta = 1.5 \times 10^{-3}$ and 3×10^{-3} cm. The resulting ratios F_f/F are listed in Table V.

To illustrate the decrement of the facilitated transport (F_f) associated with the presence of interior membranes the attenuation factor F_f (no interior membranes) $- F_f$ (n interior membranes)/F_f (no interior membranes) was computed for each combination of the above values of the parameters. The results are listed in Table VI.

DISCUSSION

An analysis of the myoglobin-mediated transport of oxygen in the presence of membranes impermeable to the carrier will be presented. These results apply to other carrier-mediated transport systems provided that the diffusion coefficients of the carrier and of the substrate-carrier complex are essentially the same (11).

TABLE IV
DEPENDENCE OF THE FACILITATED FLOW ON THE LOCATION OF THE MEMBRANES

	$F \times 10^{10}$ mol/cm^2 s	$F_f \times 10^{10}$ mol/cm^2 s	$\frac{F_f}{F}$
No interior membranes	9.1637	1.1649	0.1271
Five interior membranes near $z = 0$	9.1335	1.1347	0.1242
Five interior membranes near $z = \ell$	8.4060	0.4072	0.0484

$C_p = 8.92 \times 10^{-7}$ mol cm^{-3}, $D_1 = 1.5 \times 10^{-5}$ cm^2 s^{-1}, $D_2 = 2.7 \times 10^{-7}$ cm^2 s^{-1}, $x_1^0 = 40$ torr, $x_1^\ell = 0.5$ torr, $\ell = 10$ μm. The values of the other parameters k', k and α are listed in Table I.

TABLE V
VALUES OF F_f/F FOR A SLAB WITH n INTERIOR MEMBRANES

	$D_2 \times 10^7$ (cm^2 s^{-1}) =			2.7	2.7	2.7	2.0	2.0
	x_1^g (torr) =			0	0.1	1.0	0.1	1.0
	x_1^0 (torr)	n	δ (μm)					
ℓ = 180 μm	40	0		0.119	0.115	0.0840	0.0877	0.0638
	40	5	30	0.118	0.113	0.0832	0.0870	0.0633
	40	11	15	0.113	0.110	0.0812	0.0849	0.0620
	10	0		0.328	0.317	0.246	0.256	0.195
	10	5	30	0.320	0.310	0.242	0.252	0.192
	10	11	15	0.310	0.301	0.236	0.245	0.188
ℓ = 360 μm	40	0		0.122	0.117	0.0851	0.0892	0.0646
	40	11	30	0.119	0.114	0.0837	0.0878	0.0637
	40	23	15	0.114	0.110	0.0814	0.0854	0.0623
	10	0		0.330	0.319	0.247	0.258	0.196
	10	11	30	0.321	0.311	0.242	0.252	0.192
	10	23	15	0.310	0.301	0.236	0.245	0.188

The values of the parameters are related to Wittenberg et al. (38) experiments on bundles of pigeon breast muscle. The membranes are equally spaced, δ stands for the intermembrane distance. $C_p = 4.46 \times 10^{-7}$ mol cm^{-3}, $D_1 = 1.5 \times 10^{-5}$ cm^2 s^{-1}, the values of k', k and α are listed in Table I.

A General Expression for the Facilitated Flow

Since F is a constant, one can integrate Eq. 12 on the open interval $z_{i-1} < z < z_i$ to obtain

$$-F(z_i - z_{i-1}) = D_1[x_1(z_i) - x_1(z_{i-1})] + D_2[x_2(z_i^-) - x_2(z_{i-1}^+)]. \quad (14)$$

By summing over $i = 1, 2, \ldots, n+1$, one obtains

$$F = \frac{D_1}{\ell}[x_1(0) - x_1(\ell)] + \frac{D_2}{\ell}\sum_{i=1}^{n+1}[x_2(z_{i-1}^+) - x_2(z_i^-)]. \quad (15)$$

Observe that the quantity

$$\sum_{i=1}^{n+1}[x_2(z_{i-1}^+) - x_2(z_i^-)]$$

measures the total change of the continuous part of the function $x_2(z)$ on the interval $0 \le z \le \ell$ (cf. Figs. 1 and 2). From Eqs. 10 and 11, the second term on the right side of Eq. 15 equals the facilitated flow. One observes that what determines the transport is the change of the continuous part of the concentration function. When there are no interior membranes, the function $x_2(z)$ is continuous throughout the interval $0 \le z \le \ell$, and the second term on the right side of Eq. 15 reduces to the known expression $D_2[x_2(0) - x_2(\ell)]/\ell$ (20, 39). Thus the second term on the right side of Eq. 15 generalizes the expression $D_2[x_2(0) -$

TABLE VI
VALUES OF THE ATTENUATION FACTOR* COMPUTED FROM THE SAME RUNS OF TABLE V

	$D_2 \times 10^7$ (cm^2 s^{-1}) =			2.7	2.7	2.7	2.0	2.0
	x_1^g (torr) =			0	0.1	1.0	0.1	1.0
	x_1^0 (torr)	n	δ (μm)					
ℓ = 180 μm	40	5	30	0.0131	0.0123	0.0111	0.00930	0.00895
	40	11	15	0.0504	0.0476	0.0366	0.0351	0.0298
	10	5	30	0.0336	0.0310	0.0242	0.0241	0.0203
	10	11	15	0.0774	0.0743	0.0570	0.0589	0.0483
ℓ = 360 μm	40	11	30	0.0250	0.0239	0.0181	0.0173	0.0141
	40	23	15	0.0670	0.0640	0.0472	0.0476	0.0380
	10	11	30	0.0391	0.0375	0.0291	0.0294	0.0235
	10	23	15	0.0850	0.0793	0.0626	0.0648	0.0515

The membranes are equally spaced, δ stands for the intermembrane distance.
$C_p = 4.46 \times 10^{-7}$ mol cm^{-3}, $D_1 = 1.5 \times 10^{-5}$ cm^2 s^{-1}, the values of k', k and α are listed in Table I.
*F_f (no interior membranes) $- F_f$ (n interior membranes)/F_f (no interior membranes).

$x_2(\ell)]/\ell$ to the case of piecewise continuous concentration profiles.

By rearranging terms in Eq. 15 one obtains

$$F = \frac{D_1}{\ell}[x_1(0) - x_1(\ell)] + \frac{D_2}{\ell}\left\{[x_2(0) - x_2(\ell)] - \sum_{i=1}^{n}[x_2(z_i^-) - x_2(z_i^+)]\right\}.$$

By using Eqs. 10 and 11 and adding and subtracting $x_2^{eq}(x_1^0)$ and $x_2^{eq}(x_1^\ell)$ the following expression is obtained:

$$F_f = \frac{D_2}{\ell}\left[x_2^{eq}(x_1^0) - x_2^{eq}(x_1^\ell) - \left\{x_2^{eq}(x_1^0) - x_2(0) + \sum_{i=1}^{n}[x_2(z_i^-) - x_2(z_i^+)] + x_2(\ell) - x_2^{eq}(x_1^\ell)\right\}\right]. \quad (16)$$

For the given boundary conditions, the number $D_2[x_2^{eq}(x_1^0) - x_2^{eq}(x_1^\ell)]/\ell$ gives the maximum attainable facilitated flow. The terms under the summation sign are the values of the jump discontinuities of x_2 at the interior membranes. Since the terms $x_2(z_i^-) - x_2(z_i^+)$ could be written as $x_2(z_i^-) - x_2^{eq}[x_1(z_i)] + x_2^{eq}[x_1(z_i)] - x_2(z_i^+)$, then the first and the last differences inside the curly braces conceptually represent similar differences at the boundaries, see Figs. 1 and 2. Let

$$\Delta_i^+ = x_2^{eq}[x_1(z_i)] - x_2(z_i^+) \quad \text{and} \quad \Delta_i^- = x_2(z_i^-) - x_2^{eq}[x_1(z_i)].$$

The value for $\Delta_i^-(\Delta_i^+)$ represents the difference between the actual value of x_2 at the left side (right side) of the ith membrane and the value of x_2 that would be in chemical equilibrium with the actual value of x_1 at the same location.

Then Eq. 16 can be written as

$$F_f = \frac{D_2}{\ell}\left[x_2^{eq}(x_1^0) - x_2^{eq}(x_1^\ell) - \left\{\Delta_o^+ + \sum_{i=1}^{n}(\Delta_i^- + \Delta_i^+) + \Delta_{n+1}^-\right\}\right]. \quad (17)$$

On the interval $z^\# < z < z_i$ let the flow of the combined oxygen be transferred to the flow of the dissolved oxygen. Eq. 13 expresses this transfer as the integral

$$\int_{z^\#}^{z_i}[k'x_1(z) + k]\{x_2(z) - x_2^{eq}[x_1(z)]\}dz.$$

Observe that Δ_i^- is the second factor of the integrand evaluated at z_i. Therefore Δ_i^- is associated with the magnitude of the transfer from F_c to F_d that attends the presence of a membrane at z_i. Similarly Δ_i^+ is associated with the magnitude of the transfer of flows at the right of the ith membrane.

A mathematical analysis of the transfer of flows in the vicinity of each membrane, their relationship to the values $\Delta_i^\pm$, as well as their integration for the overall determination of the facilitated flow will be developed in a future paper.

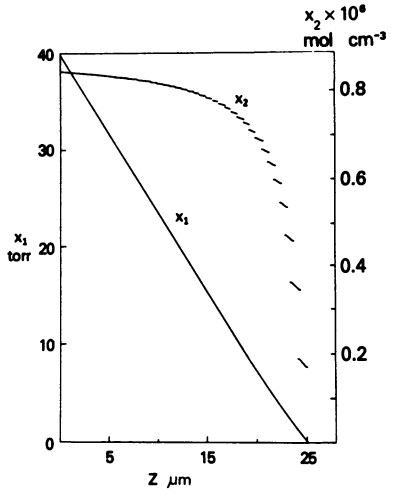

FIGURE 5 Profiles of $x_1(z)$ and $x_2(z)$ inside a slab with 39 interior membranes. $C_p = 8.92 \times 10^{-7}$ mol cm^{-3}, $D_1 = 1.5 \times 10^{-5}$ cm^2 s^{-1}, $D_2 = 2.7 \times 10^{-7}$ cm^2 s^{-1}, $x_1^0 = 40$ torr, $x_1^\ell = 0.04$ torr and $\ell = 25$ μm. The values of the other parameters k', k and α are listed in Table I. The profile of $x_1(z)$ is steeper at the membranes, however, this is not apparent in the graphs because of the lack of resolution of the scales used. For no interior membranes $F = 3.940 \times 10^{-10}$ mol cm^{-2} s^{-1} and $F_f = 7.032 \times 10^{-11}$ mol cm^{-2} s^{-1}. For 39 interior membranes $F = 3.389 \times 10^{-10}$ mol cm^{-2} s^{-1} and $F_f = 1.499 \times 10^{-11}$ mol cm^{-2} s^{-1}. This amounts to 79% decrement in the facilitated flow.

One may say that the values $\Delta_i^\pm$ represent the cost in gradient incurred by the transfer of flows imposed by the presence of a membrane at z_i. Eq. 17 can then be interpreted as follows. The facilitated flow is determined by the maximum possible difference $x_2^{eq}(x_1^0) - x_2^{eq}(x_1^\ell)$, established a priori by the boundary conditions, minus the cumulative effect of the cost attending the transfer of flows in the vicinity of each membrane.

The total change of the continuous part of the function $x_2(z)$ and the cumulative cost of the transfer of flows are complementary concepts. The former identifies the gradient that determines the facilitated flow, the latter identifies the cost in gradient incurred by the transfer of flows imposed by the presence of membranes.

In Fig. 5 the solutions $x_1(z)$ and $x_2(z)$ are graphed for $\ell = 25$ μm and 39 interior membranes. By comparing them with the ones of Figs. 1 and 2 it appears that when the number of interior membranes increases, the functions $x_1(z)$ tend to the straight line $x_1^0 - (x_1^0 - x_1^\ell)z/\ell$ and the steplike functions $x_2(z)$ tend to the x_2^{eq} of those values. However, the sum of all the differences $\Delta_i^\pm$ tends to $x_2^{eq}(x_1^0) - x_2^{eq}(x_1^\ell)$ and then by Eq. 17 the value of F_f tends to zero. This limiting case corresponds to the spatial fixation of the molecules of myoglobin with the attending chemical equilibrium and the abolition of facilitated transport.

Received for publication 13 August 1979 and in revised form 12 May 1981.

REFERENCES

1. Antonini, E., and M. Brunori. 1971. Hemoglobin and Myoglobin in Their Reactions with Ligands. Elsevier/North-Holland Publishing Co., Amsterdam.
2. Chance, B., B. Schoener, and F. S. Schindler. 1964. The intracellular oxidation-reduction state. *In* Oxygen in the Animal Organism. F. Dickens and E. Neil, editors. Pergamon Press, Oxford. 367–388.
3. Chance, B. 1964. Discussion. *In* Oxygen in the Animal Organism. F. Dickens and E. Neil, editors. Pergamon Press, Oxford. 351–352.
4. Duling, B. R. 1972. Microvascular responses to alterations in oxygen tension. *Circ. Res.* 31:481–489.
5. Duling, B. R. 1980. Coordination of microcirculatory function with oxygen demand in skeletal muscle. *In* Cardiovascular Physiology. Microcirculation and Capillary Exchange. Vol. 7. A. G. B. Kovach, J. Hamar, and L. Szabo, editors. Budapest Akademiai Kiado. Pergamon Press, New York. 1–16.
6. Duling, B. R., and R. M. Berne. 1970. Longitudinal gradients in periarteriolar oxygen tension. *Circ. Res.* 37:325–332.
7. Goldfisher, S. 1967. The cytochemical localization of myoglobin in striated muscle of man and walrus. *J. Cell Biol.* 34:398–403.
8. Gonzalez-Fernandez, J. M., and S. E. Atta. 1981. Transport of oxygen in solutions of hemoglobin and myoglobin. *Math. Biosci.* 54:265–290.
9. Gorczinski, R. J., and B. R. Duling. 1978. Role of oxygen in arteriolar functional vasodilation in hamster striated muscle. *Am. J. Physiol.* 235:H505–H515.
10. Grote, J., and G. Thews. 1962. Die Bedingungen für die Sauerstoff Versorgung des Herzmuskelgewebes. *Pflügers Arch. Ges. Physiol. Menschen Tiere.* 276:142–165.
11. Hearon, J. Z. 1973. Distribution of conserved species in diffusion-reaction systems. *Bull. Math. Biol.* 35:59–67.
12. Henneman, E., and C. B. Olson. 1965. Relations between structure and function in the design of skeletal muscles. *J. Neurophysiol.* 28:581–598.
13. James, N. T. 1968. Histochemical demonstration of myoglobin in skeletal muscle fibres and muscle spindles. *Nature (Lond.).* 219:1174–1175.
14. Jöbsis, F. F. 1964. Basic processes in cellular respiration. *Handb. Physiol. Respiration* (*Sect.* 3. I:) 63–124.
15. Jöbsis, F. F., and W. Stainsby. 1968. Oxidation of NADH during contractions of circulated mammalian skeletal muscle. *Respir. Physiol.* 4:292–300.
16. Kawashiro, T., W. Nüsse, and P. Scheid. 1975. Determination of diffusivity of oxygen and carbon dioxide in respiring tissue: results in rat skeletal muscle. *Pflügers Arch. Eur. J. Physiol.* 359:231–251.
17. Kreuzer, F., and L. J. C. Hoofd. 1970. Facilitated diffusion of oxygen in the presence of hemoglobin. *Respir. Physiol.* 8:280–302.
18. Krogh, A. 1919. The rate of diffusion of gases through animal tissues, with some remarks on the coefficient of invasion. *J. Physiol. (Lond.).* 52:391–408.
19. Krogh, A. 1919. The number and distribution of capillaries in muscles with calculations of the oxygen pressure head necessary for supplying the tissue. *J. Physiol. (Lond.).* 52:409–415.
20. Kutchai, H., J. A. Jacquez and F. J. Mather. 1970. Nonequilibrium facilitated oxygen transport in hemoglobin solution. *Biophys. J.* 10:38–54.
21. Landis, E. M. and J. R. Pappenheimer. 1963. Exchange of substances through the capillary walls. *Handb. Physiol. Circulation Sect.* 2. II: 961–1034.
22. Mahler, M. 1978. Diffusion and consumption of oxygen in the resting frog sartorius muscle. *J. Gen. Physiol.* 71:533–557.
23. Moll, W. 1968. The diffusion coefficient of myoglobin in muscle homogenate. *Pflügers Arch. Eur. J. Physiol.* 299:247–251.
24. Morita, S., R. G. Cassens, and E. J. Briskey. 1969. Localization of myoglobin in striated muscle of the domestic pig; benzidine and $NADH_2$-TR reactions. *Stain Technol.* 44:283–286.
25. Myers, W. W., and C. R. Honig. 1964. Number and distribution of capillaries as determinants of myocardial oxygen tension. *Am. J. Physiol.* 207:653–660.
26. Peachey, L. D. 1965. The sarcoplasmic reticulum and transverse tubules of the frog's sartorius. *J. Cell Biol.* 25:209–231.
27. Romanul, F. C. A. 1965. Capillary supply and metabolism of muscle fibers. *Arch. Neurol.* 12:497–509.
28. Rubinow, S. I., and M. Dembo. 1977. The facilitated diffusion of oxygen by hemoglobin and myoglobin. *Biophys. J.* 18:29–42.
29. Scholander, P. F. 1960. Oxygen transport through hemoglobin solution. *Science (Wash., D.C.).* 131:585–590.
30. Sendroy, J., Jr., R. T. Dillon, and D. D. Van Slyke. 1934. Studies of gas and electrolyte equilibria in blood. XIX. The solubility and physical state of combined oxygen in blood. *J. Biol. Chem.* 105:597–632.
31. Stainsby, W. 1966. Some critical oxygen tensions and their physiological significance. *In* Proceedings of the International Symposium in Cardiovascular and Respiratory Effects of Hypoxia. J. D. Hatcher and D. B. Jennings, editors. S. Karger, Basel. 29–40.
32. Starlinger, H., and D. W. Lübbers. 1973. Polarographic measurements of oxygen pressure performed simultaneously with optical measurements of the redox state of the respiratory chain in suspensions of mitochondria under steady-state conditions at low oxygen tension. *Pflügers Arch. Eur. J. Physiol.* 341:15–22.
33. Thews, G. 1960. Ein Verfahren zur Bestimmung des O_2-diffusion-Koeffizienten, der O_2-Leitfähigkeit und des O_2-Löslichkeitskoefficienten im Gehirngewebe. *Pflügers Arch. Ges. Physiol.* 271:227–244.
34. Whalen, W. I., and P. Nair. 1970. Skeletal muscle pO_2: effect of inhaled and topically applied O_2 and CO_2. *Am J. Physiol.* 218:973–980.
35. Wittenberg, J. B. 1959. Oxygen transport; a new function proposed for myoglobin. *Biol. Bull. (Woods Hole)* 117:402.
36. Wittenberg, J. B. 1966. The molecular mechanism of hemoglobin-facilitated oxygen diffusion. *J. Biol. Chem.* 241:104–115.
37. Wittenberg, J. B. 1970. Myoglobin-facilitated oxygen diffusion: role of myoglobin in oxygen entry into muscle. *Physiol. Rev.* 50:559–636.
38. Wittenberg, B. A., J. B. Wittenberg, and P. R. Caldwell. 1977. Role of myoglobin in the oxygen supply to red skeletal muscle. *J. Biol. Chem.* 250:9038–9043.
39. Wyman, J. 1966. Facilitated diffusion and the possible role of myoglobin as a transport mechanism. *J. Biol. Chem.* 241:115–121.